Energy Dissipation in Particle-based Impact Damper Systems: Investigation based on Elasto-plastic impact model

ME701L Term project report

R.Vishwanath (CE20B024)

Indian Institute of Technology Tirupati, India

Abstract

In this work, the non-linear dynamics of the particle damper system subject to impact load is assessed by employing the elasto-plastic model, which is used to accurately predict energy losses during a collision. Using the model, energy dissipation and other system characteristics of the particle damper system are studied, and the damping performance of the system is evaluated.

Keywords: Non-linear dynamics, Granular systems, Particle-based dampers, Contact Mechanics

1. Objectives

The objectives of this study are presented below,

1. Develop a MATLAB program based on a multi-timestep DEM framework to study inter-particle and particle-wall interaction.
2. Incorporate the elasto-plastic impact model into the viscoelastic Hertzian contact framework employed in the aforementioned MATLAB program,
3. Qualitatively assess the elasto-plastic impact model,
4. Quantitatively investigate the energy dissipation behaviour of a steel ball enclosed within a small cavity in response to a short and strong impulse load and compare the results to relevant results reported in the literature.
5. Analyse the sensitive dependence of the system response on the initial condition.

2. Overview

The attenuation of excessive vibration is a necessity in many applications. Special devices for damping/attenuating vibration are integrated within the system to ensure ergonomic comfort, protect machinery, or stabilize structures against dynamic loads. Depending on the application, the damper can be chosen. Particle dampers are a recent class of dampers. They are particularly preferred for applications requiring reduced mass. Particle-based damper systems rely on inter-particle contact and contact between particles and the wall surfaces to dissipate energy. The energy is dissipated in the form of heat and sound. Similar

to viscous dampers, these systems are used to reduce the amplitude of vibration. But mathematically, the equations of motions of particle-based systems are distinctly different as the system in case of particle impact is non-linear owing to particle contact, and the interaction between the system and its constituents is discontinuous. The energy dissipation mechanism could be very different depending on the number of particles employed and other system characteristics. Depending on the dominant mode of energy loss, particle-based dampers are classified as particle impact dampers and particle dampers in general. Energy is predominantly lost through particle wall interaction in the former [1] and inter-particle interaction in the latter [2].

Li et al. studied the irreversible energy transfer or dissipation of the system's energy to very short impulse loads ($\sim 10^{-3}$ s). Through their study, they observed that the damping performance of the system is very sensitive to the initial topology of the structure, i.e., the initial position of the particles with respect to the cavity and assessed the efficiency of these systems for different impulse forces, dimensions of cavity and different numbers of particles. A drawback of their work is the assumption of a constant coefficient of restitution. Their study concerns a steel ball, so this assumption is unjust and unwarranted. The use of the coefficient of restitution (magnitude of the relative ratio of particle velocity before and after collision measured normal to the surface of collision) is a simplified representation to account for the energy dissipation in engineering studies. However, constant descaling of velocity is not true, particularly for metals with high yield stress, as in the case of steel. The principle of energy dissipation based on contact is based on energy dissipation due to plastic deformation of the body. For highly elastic materials like steel, it is not warranted that plastic deformation has to occur, particularly at low-impact velocities.

In this work, using the elasto-plastic impact model [3] as the basis for energy dissipation, a refined analysis of irreversible energy transfer and chattering behaviour in particle impact systems is presented and compared with results assuming energy dissipation based on the coefficient of restitution reported in the relevant literature.

3. Constitutive equations

A schematic of the system is presented in fig. 1. This section explains the details regarding the equations of motion and their basis. The equations of motion of the primary structure are given below,

$$m_{PS}\ddot{z} + C\dot{z} + Kz = F(t) + F_d(t), \tag{1}$$

where the subscript PS denotes the primary system which is to be damped, z, m_{PS}, C, K, $F(t)$, $F_d(t)$ denote the position of the centre of mass of the primary system, the mass of the primary system, external viscous damping coefficient, external spring stiffness, applied load to the system and the discontinuous load applied during contact with particle respectively.

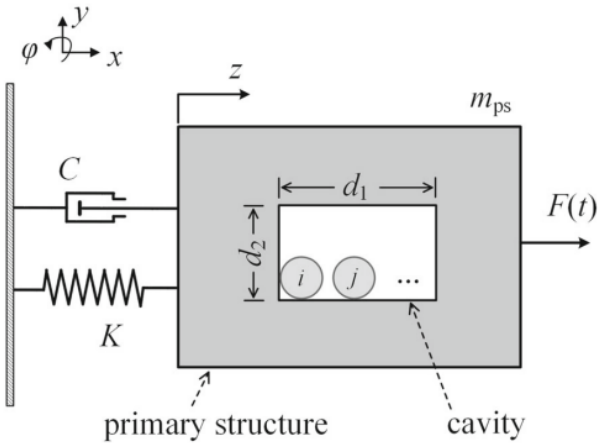

Figure 1: Schematic of system; Image taken from Li et al. [1].

The equations of motion of the particles within the cavity is given below,

$$m_i \ddot{\mathbf{u}}_\mathbf{i} = \Sigma_{j=1}^{n_p}(\mathbf{N_{ij}} + \mathbf{f_{ij}}) + \Sigma_{k=1}^{n_w}(\mathbf{N_{ik}} + \mathbf{f_{ik}}), \tag{2}$$

$$I_i \ddot{\theta}_\mathrm{i} = R_i \Sigma_{j=1}^{n_p}(\mathbf{n_{ij}} \times \mathbf{f_{ij}}) + R_i \Sigma_{k=1}^{n_w}(\mathbf{n_{ik}} \times \mathbf{f_{ik}}), \tag{3}$$

where u_i, θ_i, m_i, I_i, R_i, N_{ij}, f_{ij}, n_{ij}, n_p and n_w denote the position of the particle, rotation of the particle with respect to its centre, mass, the moment of inertia, the radius of the i^{th} particle, normal, frictional forces, relative normal distance between particles i and j, the total number of particles and the total number of wall surfaces in the primary system. Hertzian contact law is used to model the normal forces. The relation is given below

$$\mathbf{N_{ij}} = -(A_{ij}\delta_{n,ij}^{3/2})\mathbf{n_{ij}}, \tag{4}$$

where $\delta_{n,ij}$ correspond to the overlap between particles i and j (i.e. $\delta_{n,ij} = max(R_i + R_j - |\boldsymbol{u_i} - \boldsymbol{u_j}|, 0)$) and the relation for A_{ij} is given below,

$$A_{ij} = \frac{4}{3} E_{ij}^* R_{ij}^*, \tag{5}$$

$$\frac{1}{E_{ij}^*} = \frac{1-\nu_i^2}{E_i} + \frac{1-\nu_j^2}{E_j}, \tag{6}$$

$$\frac{1}{R_{ij}^*} = \frac{1}{R_i} + \frac{1}{R_j}. \tag{7}$$

In eq. (6), ν_i refers to poisons ratio of the i^{th} particle and in eq. (1), $F_d(t) = -\Sigma_{k=1}^{n_w}(\mathbf{N_{ik}} + \mathbf{f_{ik}})$. In this work, one-dimensional oscillation of particles is considered, and gravity is ignored; consequently, the effects of friction are neglected ($f = 0$) as no normal force exists perpendicular to the particle's motion.

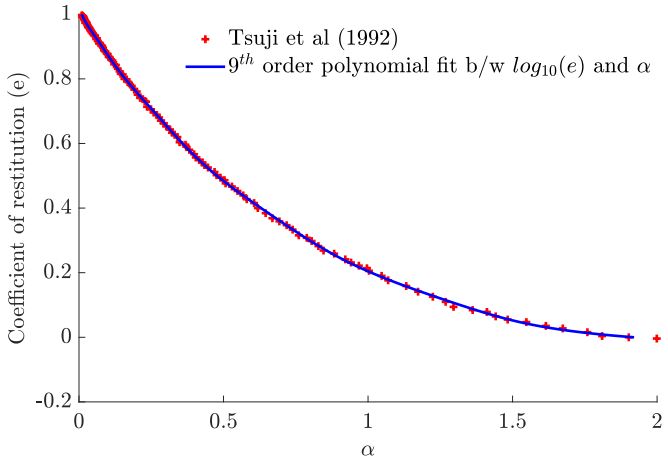

Figure 2: Curve fitting the relationship between α and coefficient of restitution (e)

3.1. Viscoelastic contact model

To model the energy losses associated with impact, Tsuji et al. proposed a viscoelastic contact model which assumes energy losses similar to viscous damping in oscillatory systems. The relation for particle contact is given below,

$$\mathbf{N_{ij}} = -(A_{ij}\delta_{n,ij}^{3/2} + \gamma_{ij}\dot{\delta}_{n,ij})\mathbf{n_{ij}}, \tag{8}$$

where γ_{ij} is given by

$$\gamma_{ij} = \alpha_n \sqrt{m_{ij}^* A_{ij}}\delta_{n,ij}^{1/4}, \tag{9}$$

$$\frac{1}{m_{ij}^*} = \frac{1}{m_i} + \frac{1}{m_j}. \tag{10}$$

In eq. (9), α is a function of the coefficient of restitution, as the formulation is based on differential equations. In their derivation, the value of α is dictated by the requirement that the ratio of particle velocity magnitude after and before impact (against a rigid surface) is equal to the coefficient of restitution. Here, the model is simplified by employing the parameter α as a function of the coefficient of restitution (e). A 9^{th} order polynomial fit between $log_{10}(e)$ and γ is employed, and the comparison of results from the polynomial fit is shown in fig. 2.

3.2. Elasto-plastic impact model

Elasto-plastic impact model proposed by Jackson et al., models the particle contact with a rigid body by considering the deformation of the particle in the elastic and plastic (assumed perfectly plastic) phases and dissipating energy based on the deformation only in the plastic phase. They also provided empirical relations to match the results based on their original model (which does not have closed-form relations).

These empirical fits are employed in this work to relate the coefficient of restitution to the impact velocity during collisions. The relation is presented below,

$$e = \begin{cases} 1 & \text{if } 1 > V_1^* > 0 \\ 1 - 0.1ln(V_1^*)\left(\frac{V_1^*-1}{59}\right)^{0.156} & \text{if } 60 > V_1^* \geq 1 \\ 1 - 0.1ln(60) - 0.11ln\left(\frac{V_1^*}{60}\right)(V_1^* - 60)^{2.36\epsilon_y} & \text{if } 1000 > V_1^* \geq 60. \end{cases} \tag{11}$$

$$V_1^* = \frac{V_1}{V_c}, \tag{12}$$

$$V_c = \sqrt{\frac{4\omega_c P_c}{5m^*}}, \tag{13}$$

$$\omega_c = \left(\frac{\pi \dot{C}_k S_{y,k}}{2E^*}\right)^2 R^*, \tag{14}$$

$$P_c = \frac{4}{3}\left(\frac{R^*}{E^*}\right)^2 (\frac{\pi}{2} C_k S_{y,k})^3, \tag{15}$$

$$C_k = 1.295e^{0.736\nu_k}, \tag{16}$$

where $S_{y,k}$, $\epsilon_{y,k}$, V_c, P_c and ω_c refer to the yield stress, critical strain where the material yields ($\epsilon_{y,k} = \frac{S_{y,k}}{E_k}$), critical velocity below which the collision is purely elastic, critical load associate with V_c and the maximum deformation or interference observed in the colliding bodies. The subscript k in the above equations denote the material that yields first. If the material of colliding bodies is distinct, the material that yields first is identified by comparing the product CS_y of each material and the material with the lowest value yields first and is denoted by subscript k in the above equations.

3.3. Summary of steps in numerical model

The system is simulated based on the DEM framework presented in fig. 3. Upon contact, the value of the coefficient of restitution corresponding to the particular impact is assessed as per eqs. (11) to (16) and the corresponding value of γ for the impact is computed based on the polynomial fit reported in fig. 2 and is substituted in eq. (8), the positions are updated and the iteration is advanced to next time step based on the time-stepping scheme.

4. Numerical methodology

4.1. DEM framework

Discrete element modelling (DEM) is a procedure to study the dynamic behaviour of particles. Each particle's motion equation is governed by its interaction with its contiguous particles. DEM is popularly

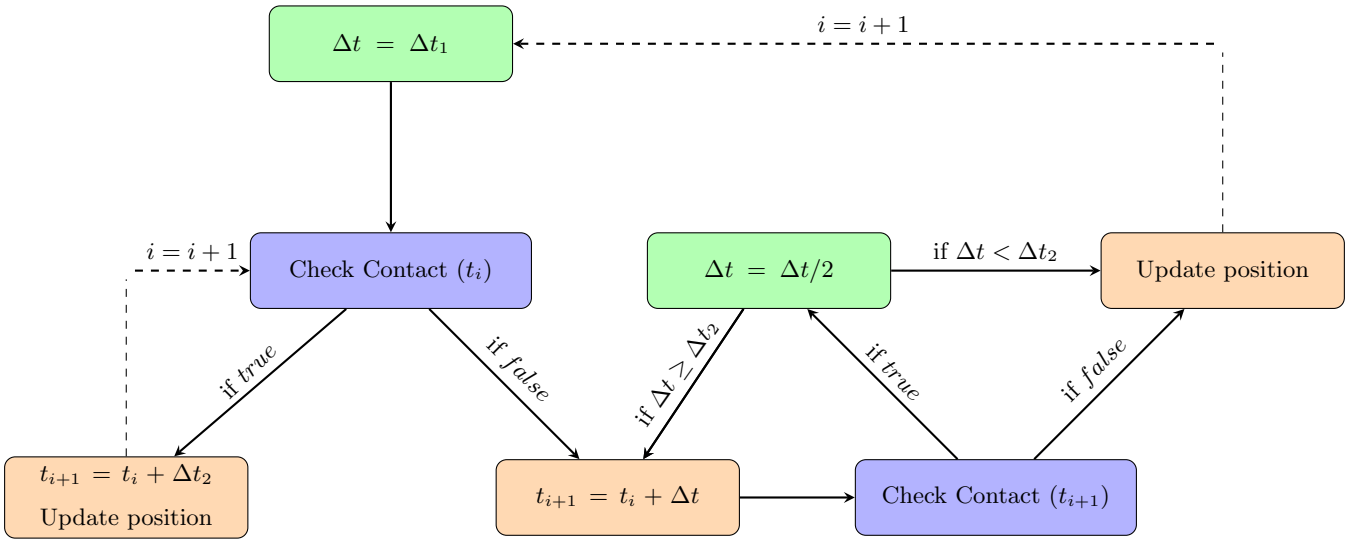

Figure 3: Framework for variable time step scheme

relied upon as a tool to study the flow of granular mechanics. Finite element modelling and other continuum-based models require the continuity of the geometry or/and continuous dependence of the constitutive equations on the local geometry. Their reliance on continuity limits their use in multi-particle systems, where the dynamics and global geometry of the system are discontinuous [5]. In this work, a multi-time step method is employed with a longer timestep for the motion of the body where the bodies are not in contact and a smaller time step when the bodies are in contact. The framework for the multistep time scheme is presented in fig. 3. In this work, ODE45 is employed as the numerical scheme for advancing the solution; as the specific timestep is provided to the function but still the timestep of the actual solver is restricted in ODE45, the actual timestep considered by the solver can be much lower than that presented in table 1. To make the solver scheme more efficient, a multistep method like the Runge-Kutta scheme can be employed instead so that an independent user control of timestep is possible.

4.2. Validation of DEM benchmarks

The simulations of Li et al. [1] for a single granule system are repeated to validate the MATLAB code written as a part of this work. For the validation, the coefficient of restitution was assumed to be uniform to maintain conformity with their work. The results are presented in fig. 4. It could be observed that the written code produces identical results to that published in [1].

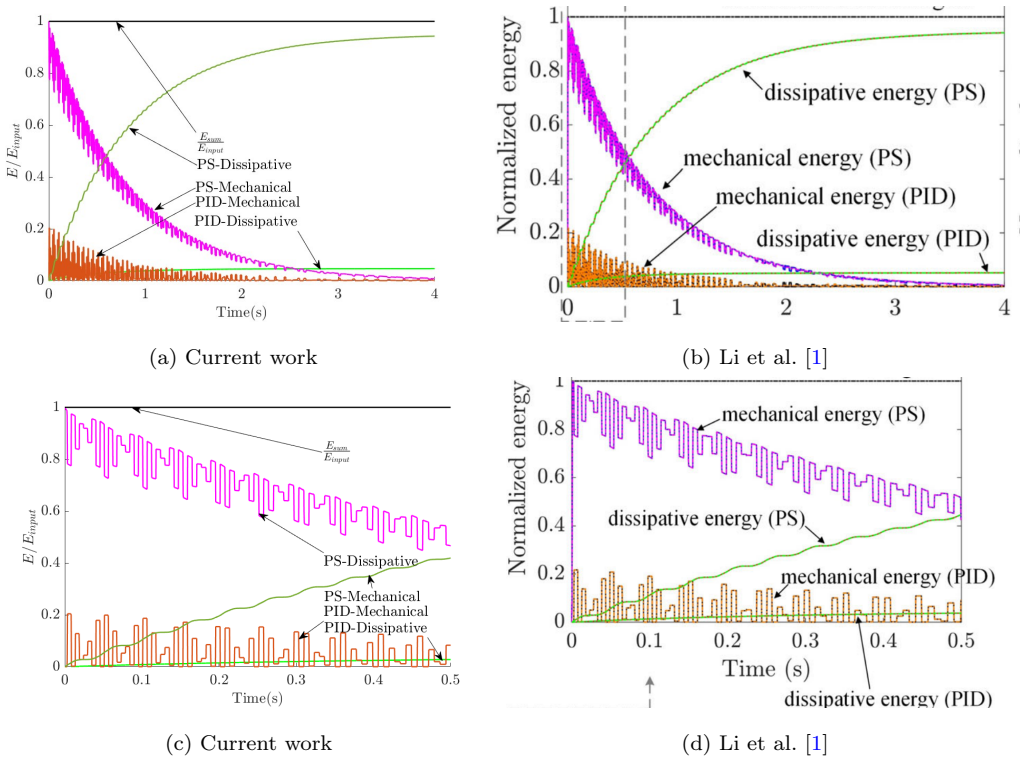

(a) Current work

(b) Li et al. [1]

(c) Current work

(d) Li et al. [1]

Figure 4: Benchmark validation: Comparison of results obtained through simulation (a,c) and results published in [1]; Simulation assumes a constant coefficient of restitution.

Table 1: Parameters employed in this study

S.no	Property	Value
1	Material	Steel
2	Modulus of elasticity	200 GPa
3	Poisson ratio	0.3
4	Yield stress	1030 MPa
5	Density	7850 kg/m^3
6	Diameter of particle	33.17 mm
7	Length of cavity	67.14 mm
8	M_{PS}	20 Kg
9	k	80000 N/m
10	Δt_1	5×10^{-6} s
11	Δt_2	3×10^{-8} s

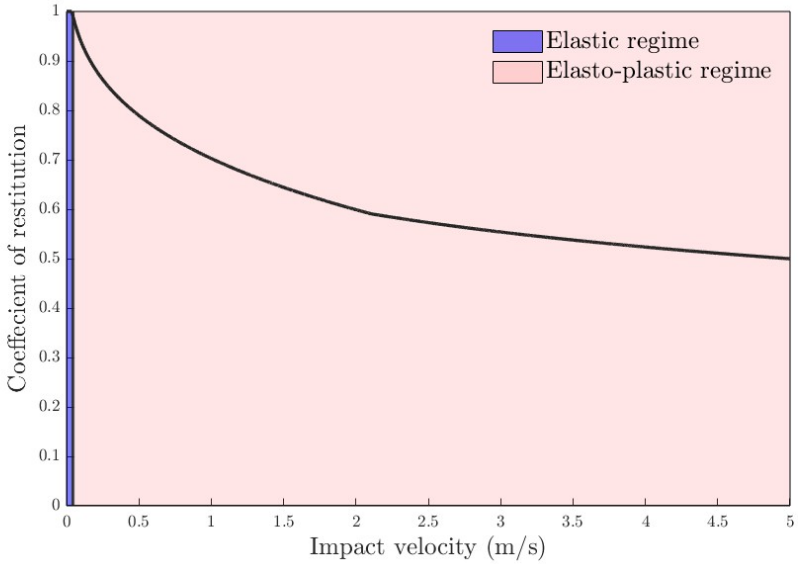

Figure 5: Variation of coefficient of restitution with the impact velocity

4.3. Parameters used in the study

The parameters used in this study are presented in table 1. Other parameters (c, F) are varied in the study and are explained in the relevant results section. Notably, the particle's mass is fixed as 6% of the mass of the primary system in this work. For the parameters assumed in the study, The variation of the coefficient of restitution with the impact velocity is shown in fig. 5

5. Results

To understand the elasto-plastic impact model, the phase portrait of a particle trapped in a fixed cavity ($k = \infty$) is presented in fig. 6. In the figure, we can observe two zones: the elastic and perfectly plastic zones. For impact in the plastic zone (corresponding to $V_1^* > 1$ in eq. (11)), the particle continues to dissipate energy due to plastic deformation (as observed by the decrease in kinetic energy). In the elastic zone (corresponding to $V_1^* < 1$ in eq. (11)), the particle undergoes continuous oscillation without energy dissipation. For any positive value of s_y, there will still be both elastic and plastic regions. Hence, the bifurcation plot is avoided here.

5.1. Irreversible energy transfer

In this section, we investigate the impact of considering the elasto-plastic model on the irreversible energy transfer occurring in the system. The plot of the evolution of instantaneous energy of the system considering the elasto-plastic impact model is presented in fig. 7a and the system assuming a constant

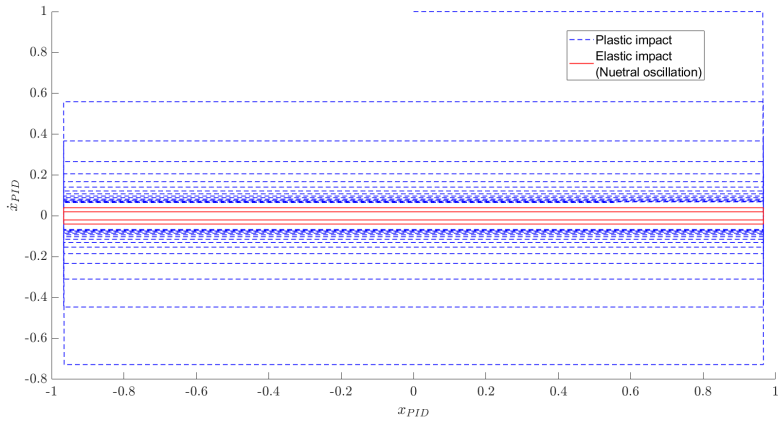

Figure 6: Phase portrait of the particle; the cavity is considered to be fixed ($K = \infty$) and of length 2 units.

coefficient of restitution of value ~ 0.99 ($\gamma = 0.006313$) is presented in fig. 7b, respectively. The initial condition of the system is set the same as case-1 in fig. 8, the damping coefficient is taken as 25.3 Ns/m and is subject to impact harmonic load as shown below

$$F = \begin{cases} F_0 sin(\frac{\pi t}{t_f}) & \text{if } t_f > t > 0, \\ 0 & \text{else,} \end{cases} \tag{17}$$

where F_0 is assigned a value of 5000N and t_f a value of 10^{-3} s. Comparing fig. 7a and fig. 7b, we can observe that in the case of the former, the instantaneous energy of the PS is smoother at later time instants ($t > 2$ s) as the particle damper dissipates energy at a much faster rate, this can be reinforced by observing fig. 7c which shows the transient plot of energy dissipated by particle impact damper in both models (for formulations related to instantaneous and dissipated energy, refer [1]). From the plot, we can observe that the system dissipates energy faster (around 100 times faster) while considering the elasto-plastic impact model. This is possibly owing to the low coefficient of restitution at high-impact velocities, which would be observed in the case of impulse loads. Upon a few contacts, the particle loses a significant portion of its impact velocity, beyond which not much energy loss is observed due to the high value of the coefficient of restitution at lower velocities.

To study the dependence of the system response on the initial topological configuration of the system, the results are simulated for all 3 cases (exhibited in fig. 8) are presented in figs. 7d and 7e. In fig. 7d, we compare the sensitivity of the system's behaviour to initial topological conditions. It could be observed that the elasto-plastic model is more sensitive to initial conditions in comparison to results presented by [1] (assuming a constant coefficient of restitution), owing to the fact that most of the energy loss occurs at the first few contacts and thus there is heavier dependence on the initial conditions. In case-3, for a force amplitude of 100N, no energy dissipation by the particle is not realized as the maximum response amplitude

is less than the clearance between the particle and the cavity at the initial configuration. In all simulated cases, case 2 provides the most consistent dissipation behaviour, which is also observed in the work of Li et al. [1].

A few select phase portraits of the system subjected to an impulse load of $F_0 = 100$N and $t_f = 0.001$s and with $c = 25.3$Ns/m are presented in fig. 9. In fig. 9a, the plot between the relative position and the relative velocity of the particle w.r.t primary system is presented for different initial conditions and in fig. 9b, the plot between the position and corresponding instantaneous velocity of the primary system are presented. For case-1, we observe a pure, stable focus at the centre, as in this case, the maximum amplitude is smaller than the clearance in the cavity ($d_0 = 0.4$mm); thus, the particle never makes contact with the primary system, and the stable convergence is due to the viscous damping of the primary system. Due to particle contact, the system behaviour is fundamentally different for the other cases. It can be observed that as the velocity of the system reduces to energy loss in the collision, the relative velocity in the plot decreases. From the plot, we can observe the sensitive dependence of the system response on the initial conditions, particularly at low impulse loads, suggesting the system is chaotic. The amplitude response of the system to the impulse load in the frequency domain is plotted in fig. 10. The plot shows the response of the model considering a constant coefficient of restitution very close to 1 ($\gamma = 0.006313$) and the response while employing the elasto-plastic impact model. The latter model provides a reduced amplitude of response across all frequency ranges as the energy dissipation is very small in the former model, and consequently, a larger amplitude of motion is expected. The sharp peak observed near the origin corresponds to the natural frequency of the system ($\omega_{res} \sim 61.3$ rad/s $\approx \sqrt{\frac{k}{M_{PS}}} = 63.24$) rad/s. As it is a two-degree freedom system, another peak due to the second resonant frequency is expected at higher frequencies. The system exhibits a significant amplitude in a range of frequencies, possibly owing to chattering behaviour [6]. To finally investigate the effect of the particle damper in terms of damping performance, the plot of the amplitude response of a system with and without particle damper system is plotted in fig. 11. It could be observed that the earlier attenuation of vibration is observed in the case with the particle damper.

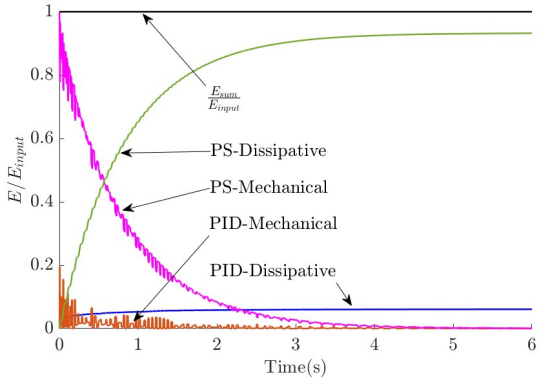

(a) Elasto-plastic impact model

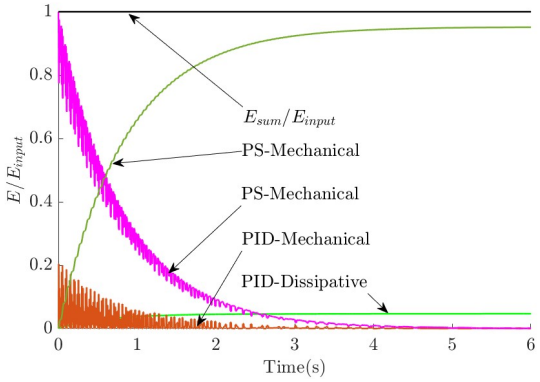

(b) Constant coefficient of restitution

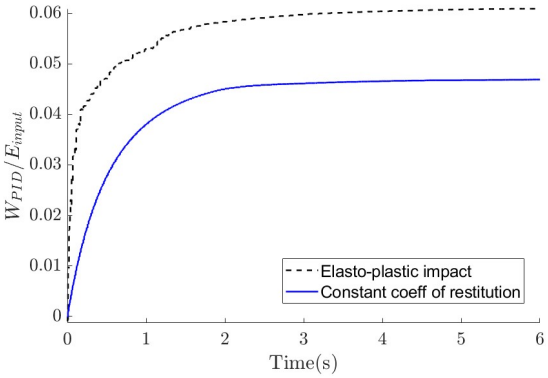

(c) Transient behaviour of energy dissipated by particle-wall collision; $F_0 = 5000N;\ t_0 = 10^{-3}\ s; Case-1$

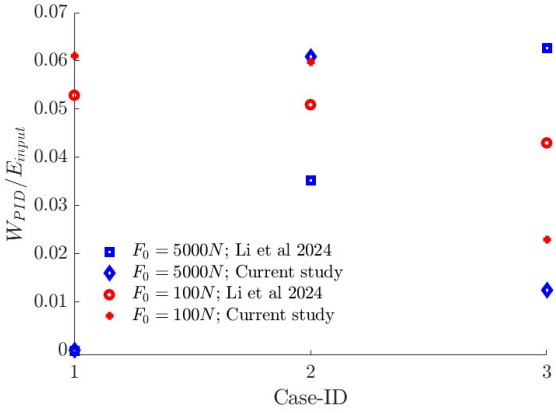

(d) Dependence of viscous energy dissipation on the initial and load condition; $F_0 = 5000N;\ t_0 = 10^{-3}\ s$; Case-1

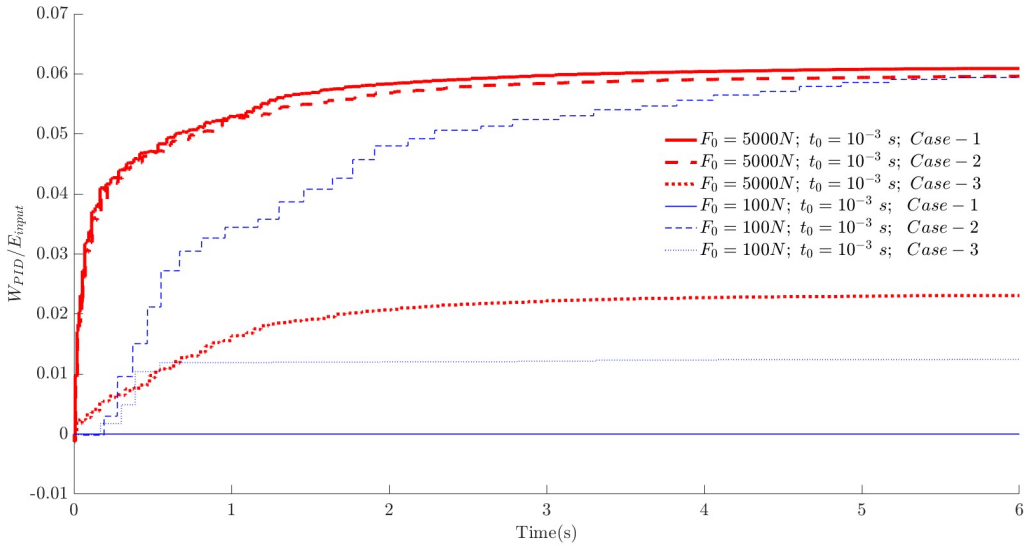

(e) Sensitivity of energy dissipation on initial condition

Figure 7: Study of irreversible energy transfer or energy dissipation; c=25.3Ns/m

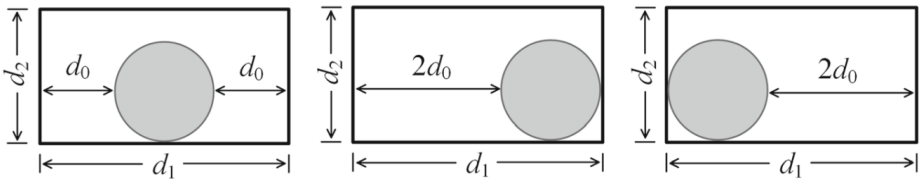

Figure 8: Initial topological configurations; Cases $1-3$ (from left to right); $d_0 = 0.4$ mm in this study; Image taken from Li et al. [1].

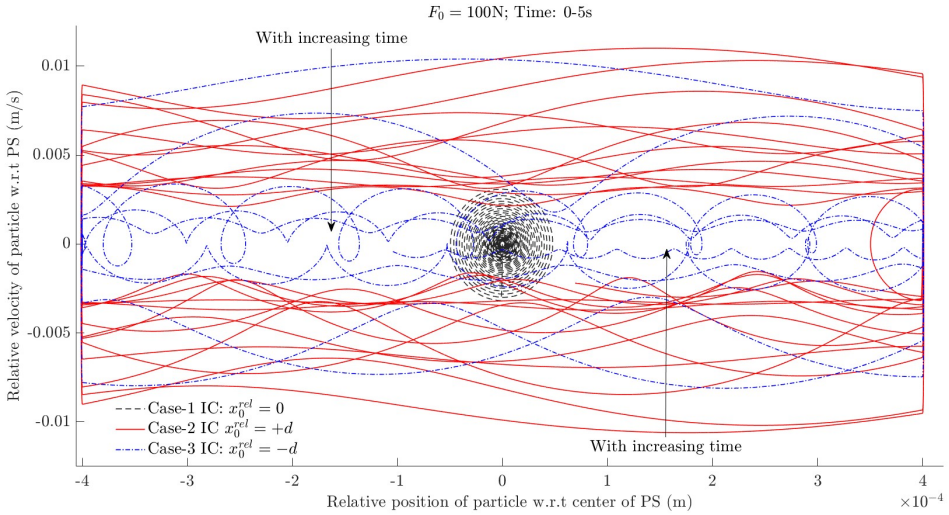

(a) Plot of the relative position of the particle within the cavity against the corresponding relative velocity of the particle for different initial positions; Impulse load conditions: $F_0 = 100N$ and $t_f = 0.001$s;

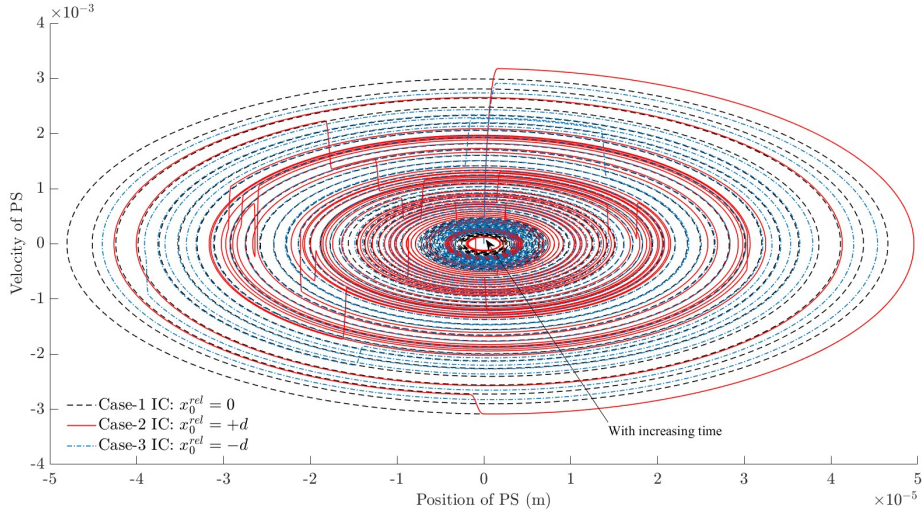

(b) Plot of the position of the primary system within the cavity against the corresponding velocity of the primary system for different initial conditions; Impulse load conditions: $F_0 = 100N$ and $t_f = 0.001$s;

Figure 9: Few select phase portraits of the system

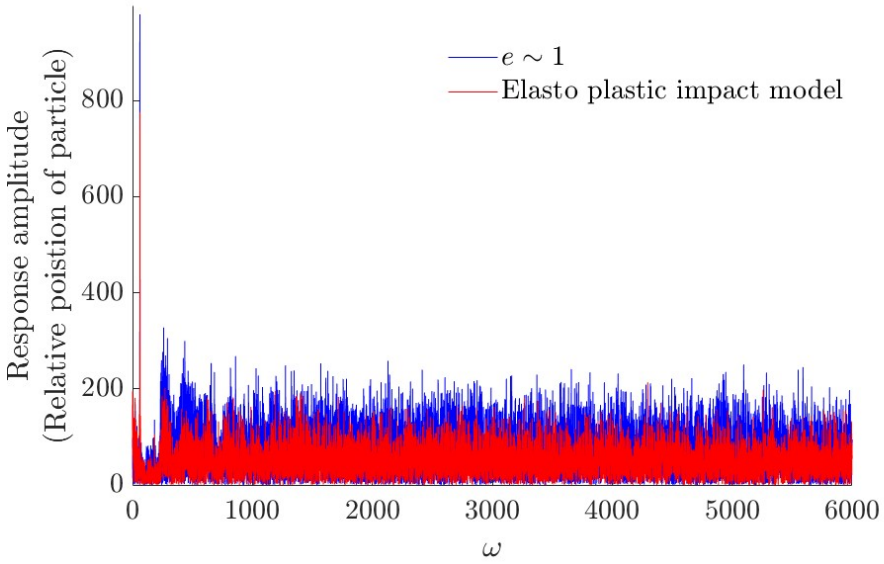

(a) Amplitude response of the particle (w.r.t primary system) in the frequency domain; Impulse load conditions: $F_0 = 5000N$ and $t_f = 0.001$s; System conditions: case-1;

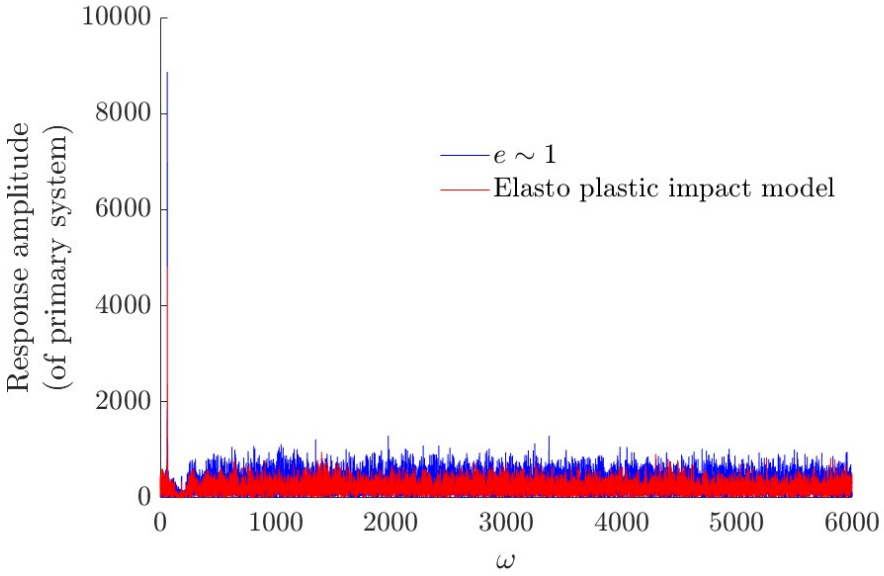

(b) Amplitude response of the primary system in the frequency domain; Impulse load conditions: $F_0 = 5000N$ and $t_f = 0.001$s; System conditions: case-1;

Figure 10: Analysis of system behaviour in the frequency domain

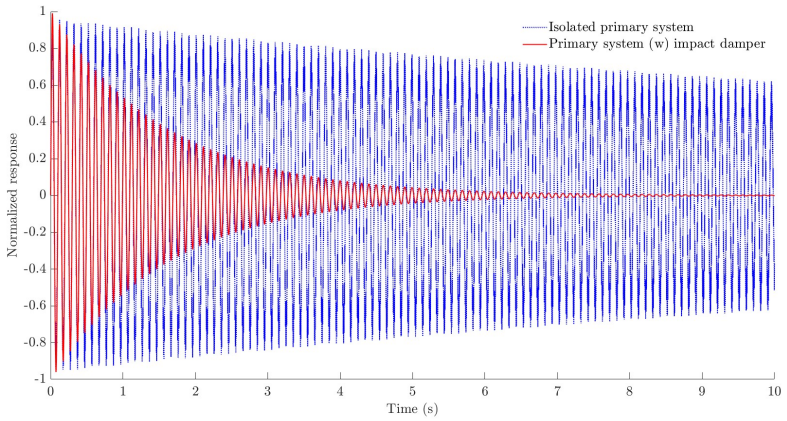

Figure 11: Damping characteristics of the system; Impulse load conditions: $F_0 = 100N$ and $t_f = 0.001$s; system conditions: $c = 25.3$Ns/m and initial condition: case 3;

6. Conclusion and perspectives

In this work, the damping performance of the particle damper system subject to impact load is assessed by employing the elasto-plastic model to accurately predict energy losses during a collision. The key takeaways of the work are listed below,

1. The qualitative phase portrait of the particle trapped in a cavity is observed to have a neutral oscillation in the elastic phase and energy dissipation in the elastic phase (Refer fig. 6).
2. The energy dissipation in the work of Li et al. is observed to be an underestimation as they assumed a constant coefficient of restitution which is near unity (Refer figs. 7a to 7c), but for impulse loads due to the high variability in the impact velocities and consequently the coefficient of restitution for each contact is vastly different (Refer fig. 5).
3. Similar to observations made in Li et al. [1], the energy dissipation is observed to be sensitive to the initial topology of the system (Refer figs. 7d and 7e). A few select phase portraits are further plotted to confirm the chaotic behaviour of the system (Refer fig. 6).
4. The response of the system in the frequency domain is investigated (Refer fig. 10).
5. The performance of the particle damper system in damping performance is studied (Refer fig. 11).

6.1. Comments on non-linear characteristics exhibited by the system

Due to the short time-span of particle-wall contact, non-linear characteristics associated with the non-linear spring in Hertzian contact model is not observed. However, non-linearity associated with the discontinuity does exhibit in the form of chaotic motion where a meagre deviation of 0.4mm has been shown to cause nearly 50% drop in efficiency in terms of dissipation (Refer fig. 7e). The non-linearity associated with

the elasto-plastic impact model is not realized in this work as the time-scale studied in this work is too small for the system to reach its steady state (without eternal damping) and the particle collision observed in this study predominantly occur in the plastic regime. It is expected that the non-linear characteristics associated to elasto-plastic model would have been exhibited in the form of chattering (i.e. regularly sustained contacts within a single cycle of motion) [7], a bifurcation in the number of contacts between the particle and primary system within a single oscillation of primary system is expected with the variation of frequency of the harmonic load [8].

References

1. Li X, Mojahed A, Wang C, Chen LQ, Bergman LA, Vakakis AF. Irreversible energy transfers in systems with particle impact dampers. *Nonlinear Dynamics* 2024;112(1):35–58. URL: https://doi.org/10.1007/s11071-023-09007-3. doi:10.1007/s11071-023-09007-3.
2. Prasad B, Duvigneau F, Juhre D, Woschke E. Damping performance of particle dampers with different granular materials and their mixtures. *Applied Acoustics* 2022;200. doi:10.1016/j.apacoust.2022.109059.
3. Jackson R, Green I, Marghitu D. Predicting the coefficient of restitution of impacting elastic-perfectly plastic spheres. *Nonlinear Dynamics* 2010;60:217–29. doi:10.1007/s11071-009-9591-z.
4. Tsuji Y, Tanaka T, Ishida T. Lagrangian numerical simulation of plug flow of cohesionless particles in a horizontal pipe. *Powder Technology* 1992;71(3):239–50. URL: https://www.sciencedirect.com/science/article/pii/003259109288030L. doi:https://doi.org/10.1016/0032-5910(92)88030-L.
5. Mahmood AA, Elektorowicz M. A review of discrete element method research on particulate systems. *IOP Conference Series: Materials Science and Engineering* 2016;136(1):012034. URL: https://dx.doi.org/10.1088/1757-899X/136/1/012034. doi:10.1088/1757-899X/136/1/012034.
6. Du Y. Investigation of chattering behavior of impact damper. *Advances in Mechanical Engineering* 2017;9(12):1687814017743110. URL: https://doi.org/10.1177/1687814017743110. doi:10.1177/1687814017743110. arXiv:https://doi.org/10.1177/1687814017743110.
7. Du Y, Zhang G. Research on chattering occurrence condition in a vibro-impact system. *Journal of Low Frequency Noise, Vibration and Active Control* 2019;38(3-4):1202–13. URL: https://doi.org/10.1177/1461348418813289. doi:10.1177/1461348418813289. arXiv:https://doi.org/10.1177/1461348418813289.
8. Wang S, Luo G. Bifurcation characteristics of fundamental and subharmonic impact motions of a mechanical vibration system with motion limiting constraints on a two-parameter plane. *Shock and Vibration* 2021;2021:6634013. URL: https://doi.org/10.1155/2021/6634013. doi:10.1155/2021/6634013.